Pharmaceutical Research, Vol. 27, No. 4, April 2010 (© 2010)
DOI: 10.1007/s11095-009-0041-x

Research Paper

Micellar Nanocarriers: Potential Nose-to-Brain Delivery of Zolmitriptan as Novel Migraine Therapy

Ratnesh Jain,[1] Swapna Nabar,[2] Prajakta Dandekar,[1] and Vandana Patravale[1,3]

Received October 21, 2009; accepted December 15, 2009; published online February 12, 2010

Purpose. The investigation was aimed at developing micellar nanocarriers for nose-to-brain delivery of zolmitriptan with the objective to investigate the pathway involved in the drug transport.
Methods. The micellar nanocarrier was successfully formulated and characterized for particle size and shape by multi-angle dynamic light scattering, small angle neutron scattering and cryo-transmission electron microscopy. Toxicity and biodistribution studies were carried out in rat. The distribution of the nasally administered labeled micellar nanocarrier in various regions of the rat brain was determined using the brain localization and autoradiography studies.
Results. Micellar nanocarrier of zolmitriptan, with size of around 23 nm, was successfully formulated. The spherical nature of the nanocarrier was confirmed using DLS, SANS and cryo-TEM. Toxicity studies indicated the safety for administration in the nasal cavity. *In vivo* biodistribution studies indicated the superiority of the developed nanocarrier for brain targeting when compared with the intravenous and nasal solutions of the drug. Brain localization and autoradiography studies illustrated the distribution of the drug in various regions of the brain and revealed a possible nose-to-brain transport pathway for the labeled drug.
Conclusion. The investigation indicated the potential of the developed nanocarrier as an effective new-generation vehicle for brain targeting of zolmitriptan.

KEY WORDS: autoradiography; biodistribution; brain targeting; micellar nanocarrier; zolmitriptan.

INTRODUCTION

Zolmitriptan, a structural analogue of serotonin (5-hydroxytryptamine; 5-HT), is a selective (5-HT) 1B/1D agonist. This moiety, which belongs to the class of drugs collectively referred to as triptans, is the second molecule to be marketed after sumatriptan and has been reported to have improved pharmacokinetic properties as compared to the earlier moiety (1). This drug is prescribed for the treatment of acute migraine associated with menses, with or without aura and cluster headaches (2). Zolmitriptan mimics the action of serotonin by directly stimulating the serotonin receptors in the brain and thus leads to vasoconstriction of the blood vessels of the brain. Also, reduction in sterile inflammation associated with antidromic neuronal transmission by zolmitriptan is yet another mechanism by which it has been reported to provide relief of acute migraine attacks (3,4).

Currently, zolmitriptan is available commercially as oral tablets (conventional and orodispersible) and a nasal spray (2). Despite the fact that zolmitriptan is a potent molecule, the current oral therapies present drawbacks, such as slow onset of action, low bioavailability (40–45%), nausea and incomplete pain relief with recurrence of headaches (2,5,6). Additionally, oral zolmitriptan exhibits a short half-life of 1–2 h, with the drug undergoing first-pass metabolism and being rapidly cleared by the hepatic and the renal systems (7). Administration of the nasal solution of the drug in the spray form resulted in a quicker onset of action, providing headache relief within 15 min of administration. However, clinical evidences show no significant improvement in other pharmacokinetic parameters, such as half-life, bioavailability and therapeutic gain, over the oral dosage forms (6). Despite these limitations, reports indicate that zolmitriptan is the only triptan which, although not significantly effective in first dose, has been found to provide a relief after the administration of a second dose (8,9). This fact provides a strong rationale for designing more effective nasal dosage forms capable of directly targeting the drug to the brain to overcome the aforementioned drawbacks. Also nose-to-brain delivery of drug moieties has been attempted by several researchers to exploit the advantages of this route such as circumvention of the blood-brain barrier, avoidance of hepatic first-pass metabolism, practicality and convenience of administration and non-invasive nature (10). Researchers have attempted the formulation of mucoadhesive microemulsion dosage form of zolmitriptan. However, no definitive studies to predict the possible pathway of transfer of zolmitriptan from nose to brain have been reported (2).

Thus, the current investigation focuses on the design of novel drug delivery system for nose-to-brain administration

[1] Department of Pharmaceutical Sciences and Technology, Institute of Chemical Technology, N.P. Marg, Matunga, Mumbai 400 019, India.
[2] Radiation Medicine Centre, Bhabha Atomic Research Centre, Parel, Mumbai 400 012, India.
[3] To whom correspondence should be addressed. (e-mail: vbp_muict@yahoo.co.in)

of zolmitriptan. Micellar nanocarriers of the drug were developed to exploit their advantages, such as low particle size, enhanced permeability across nasal mucosa, suitable flow properties, and ability to incorporate varying ingredients, which would allow targeting of the solubilized moiety, longetivity and higher retention effects in the desired areas, in turn providing an enhanced drug action (11). Although micellar dosage forms have earlier been used for oral, parenteral and ocular applications (11), their application for nose-to-brain delivery is the first of its kind, to our present knowledge. The developed zolmitriptan-loaded micellar nanocarriers were characterized with respect to various physico-chemical characteristics to determine their suitability for nasal administration. Biodistribution studies were conducted with the radiolabeled, drug-loaded formulations to confirm their brain-targeting efficiency. Also, brain localization and autoradiography studies were attempted with the labeled micelles, with an aim of hypothesizing the probable pathway involved in the transfer of drug from nose to brain. Although effective in drug delivery, the nasal mucosa has been reported to be very sensitive to any foreign material instilled into the nose. Many of the permeation enhancers and mucoadhesive agents used in these formulations, as well as the drugs, may give rise to serious toxicity concerns with regards to the nasal mucosal membrane, the nasal cilia and ciliary movement, the mucus discharge and the nasal epithelial tissue (12,13). Nasal toxicity studies were thus attempted for the developed formulation to rule out its negative impacts on nasal physiology and harmful systemic effects, if any. The investigation was thus aimed at providing a completely safe and effective formulation with brain-targeting potential. Direct brain targeting was hypothesized to reduce the dose and hence the dosing frequency of the administered drug.

MATERIALS AND METHODS

Materials

Chemicals

Zolmitriptan was provided as a kind gift by Archarchem Pharmaceuticals Pvt. Ltd. (Mumbai, India). Transcutol P® (TCP, Diethylene glycol monoethyl ether) was kindly gifted by Gattefosse (Mumbai, India). Pluronic® F127 (PF127, Poly (ethylene oxide)-poly (propylene oxide) block copolymer) was generously provided by BASF India Ltd. (Mumbai, India). Vitamin E-TPGS (TPGS, d-α-Tocopheryl polyethylene glycol 1,000 succinate) was procured from Eastman Chemical Ltd. (Mumbai, India). Acetonitrile (HPLC grade) was purchased from Merck International (Mumbai, India). Polyethylene glycol-400 (PEG-400), benzyl alcohol (BA) and all other chemicals were obtained from S. D. Fine Chemicals Ltd. (Mumbai, India). All the materials were used as received without any further modifications. Ultrapure water (Milli Q Plus system, Millipore, Bedford, MA, USA) was used whenever necessary.

Animals

Animal experiments were carried out in accordance with the guidelines of the institutional ethics committee (Radiation Medicine Centre, Bhabha Atomic Research Centre, Mumbai). Male and female Wistar rats aged 6–8 weeks having body weight in the range of 275–325 g were used for the study. The animals were housed at a temperature of 22±3°C and 65% relative humidity. Throughout the experiments, the animals were fed with a standard rat diet and were provided with clean drinking water *ad libitum*.

Formulation of Micellar Nanocarrier of Zolmitriptan

Various GRAS (generally regarded as safe) approved surfactants were employed for formulating the micellar nanocarriers of zolmitriptan. To describe in brief, zolmitriptan (20 mg) was dissolved in a mixture of TCP (180 mg) and BA (100 mg). The surfactants, viz. PF127 (50 mg), PEG-400 (100 mg) and TPGS (50 mg) were dissolved together in citrophosphate buffer (pH 5.8, 500 mg). The resulting solutions were mixed together under agitation on a cyclo mixer (100 rpm, Remi CM-101, Mumbai, India) for 10 min. to obtain an optically clear formulation.

Characterization of Micellar Nanocarrier

Dynamic Light Scattering

The particle size and polydispersity index (PI) of the developed system was measured by Dynamic Light Scattering (DLS) using a Malvern Autosizer 4800 instrument (Malvern, Worcestershire, UK) employing 7132 digital correlator, at 25ºC. The light source was argon ion laser (Coherent, Innova, USA) operated at 514.5 nm with a maximum output power of 2 W. Multi-angle measurements were carried out by varying the scattering angle between 30° and 150°, whereas the routine measurements were conducted at 90°. The correlation functions were analyzed by the method of cumulants.

Small-Angle Neutron Scattering

Small-angle neutron scattering experiments were conducted on samples prepared at different dilution levels (Micelle: D_2O; 35:65, 20:80, 5:95; v/v) with and without zolmitriptan. Small-angle neutron scattering experiments for micellar nanocarrier were carried out using SANS diffractometer at Dhruva reactor, Bhabha Atomic Research Centre, Trombay. The diffractometer makes use of a beryllium oxide filtered beam of mean wavelength (λ) of 5.2 Å. The accessible wave vector transfer ($Q=4\pi\sin\theta/\lambda$, where 2θ is the scattering angle) range of the diffractometer is 0.02–0.3 Å. Samples were held in a quartz sample holder of 0.5 cm thickness. In all measurements, the temperature was kept fixed at 30°C. The measured SANS data were corrected and normalized to a cross-sectional unit, using standard procedures.

The differential scattering cross-section per unit volume [$d\Sigma/d\Omega$] for monodisperse isotropic scatterers can be written as

$$d\Sigma/d\Omega = (\Delta\rho)^2 v^2 N P(q) S(q)$$

where $\Delta\rho^2$ is the contrast factor, N is the number density of scatterers, v is the volume of the scatterer, P(q) is the form factor characteristic of specific size and shape of the scatterers

and S(q) is the structure factor that accounts for the inter-particle interaction. Further, in order to describe core radius (r), a form factor for monodisperse spheres was considered, which can be stated as

$$P(q)=[3\{\sin(qr)-qrCos(qr)\}/(qr)3]2$$

The inter-particle interaction was captured from the analytical solution of the Ornstein–Zernike equation in the Percus–Yevick approximation employing hard sphere potential (14). The total volume fraction of the micelles and the overall core and shell radius of the micelles were used as variables in S(q) calculation. Similar approach for the analysis of SANS data of block copolymer micelles has been employed by researchers earlier (14).

Cryo-transmission Electron Microscopy (cryo-TEM)

The cryo-TEM investigations were carried out with a Carl Zeiss Libra 120 transmission electron microscope (Carl Zeiss NTS, Oberkochen, Germany). The instrument was operated at 120 kV and in zero loss bright-field mode. Digital images were recorded under low dose conditions using a Gatan MultiScan 791 CCD camera (Gatan, Oxfordshire, UK) and the WinTEM software (Carl Zeiss, Oberkochen, Germany). An underfocus of 1–2 μm was used to enhance the image contrast and thus enable detailed imaging. The techniques used for sample preparation and image analysis were in accordance with published literature (15). Briefly, a small drop (~5 μL) of the sample was placed on a copper grid covered with a perforated polymer film. Excess liquid was thereafter removed by means of blotting with a filter paper, leaving a thin film of the solution on the grid. Thereafter, the sample was immediately vitrified in liquid ethane, held just above its freezing point. Care was taken to maintain the samples below −174°C and protect them from external atmospheric variations, both during transfer to the TEM as well as during analysis.

Toxicity Evaluation

Toxicity studies were conducted using Wistar rats (n=6) of either sex. The animals were divided into four groups; the first three groups were administered with the marketed formulation of zolmitriptan (equivalent to 0.3 mg/kg; Zomig®, AstraZeneca Pharmaceuticals, Banglore, India), the placebo micellar nanocarrier (equivalent to 0.3 mg/kg) and the zolmitriptan micellar nanocarrier (0.3 mg/kg), respectively. The results obtained were compared with those of the fourth group, in which no test substance was administered to the animals (negative control group). The rats were anaesthetized using ketamine (50 mg/kg) injection, administered intramuscularly. Formulations (50 μl/nostril) were instilled into nostrils with the help of Hamilton syringe (100 μL) attached with polyethylene tubing with an internal diameter of 0.1 mm. The details of the experimental design have been stated in Table I. The animals were sacrificed at each time point, and the stated parameters were evaluated. The animals were monitored for any signs of behavioral abnormalities or mortality during the course of the study.

Biodistribution Studies

The biodistribution studies were carried out in male Wistar rats divided into three different groups containing six animals each. The animals were administered nasal solution, intravenous solution and nasal micellar nanocarrier, respectively, formulated using ^{99m}Tc- zolmitriptan complex, where the drug was radiolabeled using a modified direct labeling method (16). To describe in brief, 1 ml of drug solution was (20 mg/ml) taken to which 100 μg of stannous chloride dihydrate in 100 μl of 0.1 N HCl was added, and pH was adjusted to 6.80±0.20 using 50 mM sodium bicarbonate solution. To the resultant mixture (filtered through 0.22 μm nylon membrane), 1 ml of sterile 99mTc-pertechnetate (75 to 400 MBq) was added over a period of 60 sec with continuous mixing, and the resultant mixture was incubated at 30°C±5°C for 30 min with continuous nitrogen purging. The final volume was made up to 2.5 ml using 0.90% (w/v) of sterile sodium chloride solution. The labeled drug was mixed along with other formulation excipients to result in the micellar nanocarrier. The administration and dosing details of the study protocol have been stated in Table II. The intravenous solution containing the ^{99m}Tc- zolmitriptan complex was injected through penile vein of the animals. The nasal formulations were administered in accordance with the reported experimental procedures (17), incorporating slight modifications wherever required. The formulations were instilled into the rat nostrils using Hamilton syringe fitted with polyethylene tube with internal diameter of 0.1 mm. At the end of the dosing, the rats were sacrificed at various time points (30, 60, 120 and 240 min), after anaesthesizing with ketamine intramuscular (50 mg/kg) and xylazine intraperitoneal (25 mg/kg) injections. Subsequently, brain and other body organs/tissues (e.g. heart, spleen, liver, etc.) were collected along with blood samples, collected using

Table I. Experimental Details for Toxicity Evaluation of Micellar Nanocarrier

Time point (Day/s)	Parameter(s) studied
1	Histopathology: Gross pathological changes in nasal mucosa and mucosal cilia
4	Histopathology: Gross pathological changes in nasal mucosa and mucosal cilia
7	Histopathology: Gross pathological changes in nasal mucosa and mucosal cilia
28	Histopathology: Gross pathological changes in nasal mucosa and mucosal cilia, gross pathological changes in major body organs Hematology: Haemoglobin, hematocrit, erythrocyte count (RBC), platelet count, leucocyte count, WBC count, monocyte, neutrophil, eosinophil Serum biochemistry: Albumin, globulin, blood urea nitrogen, creatinin and total protein

Table II. Study Details of Biodistribution, Brain Localization and Autoradiography Studies

Formulation	Administration	Volume	Dose	Euthanasia time points[#] (min)	Study
^{99m}Tc-Zolmitriptan Micellar	Nasal	50 µl /nostril	125 µci/100 µl +0.4 mg zolmitriptan	30, 60, 120, 240	GS
Nanocarrier	Nasal	50 µl /nostril	200 µci/100 µl +0.4 mg zolmitriptan	30, 60, 120, 240	AR BL
^{99m}Tc-Zolmitriptan Solution	Nasal	50 µl /nostril	125 µci/100 µl +0.4 mg zolmitriptan	30, 60, 120, 240	GS
	I.V.	100 µl	125 µci/100 µl +0.4 mg zolmitriptan	30, 60, 120, 240	GS

GS gamma spectrometry, *AR* autoradiography, *BL* brain Localizaton; [#] (n=6/time point)

cardiac puncture. The uptake of ^{99m}Tc-zolmitriptan was expressed as the percent of the administered dose per gram of the organ/tissue after recording the weight of the individual organs/tissues and measuring the radioactivity in each tissue/organ using well-type gamma spectrometer (Electronic Corporation of India Ltd., Mumbai, India).

Brain Localization and Autoradiography

The distribution of the nasally administered labeled micellar nanocarrier in various regions of the brain was determined using the brain localization and autoradiography studies. A higher radioactivity dose was used for the autoradiography studies to assist in visualization of the drug in various brain sub-parts. The details of the administration protocol of the test formulations have been stated in Table II. At specified time points, the rats were sacrificed and the brains were isolated using experimental procedures published earlier (18). Sections of various parts of the rat brain, including olfactory bulb (OB), frontal cortex (FC), olfactory tubercle (OT), caudaputamen (CP), hippocampus (HC), diencephalon (DC), mid brain (MB), cerebellum (CL), pons (PN) and medulla (MD), were fixed on glass slides using formaldehyde and were subsequently stained using hematoxyline-eosin. These brain sub-parts were identified according to the description and classification published by George Paxinos and Charles Watson (19). Radioactivity in different parts of the brain was counted using well-type gamma spectrometer, and percent distribution of the drug in various parts of the brain was determined.

For autoradiography, the rat brains were rapidly isolated from the bodies after sacrificing the animals by decapitation at specified time points (Table II). The brains were frozen with powdered dry ice and cut into thin sections (20 µm) using a cryomicrotome (Leica CM3050 Cryostat, Wetzlar, Germany) before thaw mounting them onto microscope slides. Various coronal and sagittal sections of rat brain were exposed to X-ray film (Fuji Film Co. Ltd., Tokyo, Japan) in an X-ray casette (Kiran X-ray, Mumbai, India) for 48 h. The X-ray film was processed, and autoradiograms were examined to evaluate the radioactivity distribution in the different brain sub-parts.

Statistical Analysis

Data was expressed as mean±S.D., and various parameters were statistically assessed by unpaired t-test using Graphpad Instat Demo version. Differences of $P<0.05$ were considered to be statistically significant.

RESULTS

Formulation of Zolmitriptan Micellar Nanocarrier

The micellar nanocarrier of zolmitriptan was formulated using PF127 in combination with PEG-400 and TPGS. The concentrations of the various formulation components were optimized depending on their ability to yield micellar nanocarrier with suitable particle size and distribution. At the same time, importance was given to the fact that the selected concentrations would completely solubilize the drug, thus affording an optically clear and transparent system.

Dynamic Light Scattering

The optimized micellar nanocarrier of zolmitriptan exhibited a particle size of 24.2±0.73 nm with a PI of 0.064± 0.037 when analyzed by Multiangle dynamic light scattering (DLS) technique. Analysis at different scattering angles revealed no significant difference in particle size (Table III), thus suggesting a homogenous and uniform nature of the developed system.

Small-Angle Neutron Scattering

The small-angle neutron scattering experiments revealed the spherical nature of the developed micelles (Fig. 1). The effect of dilution was evaluated on the core and hard sphere radius of the developed micelles. It was found that at Micelle: D_2O ratio of 35:65 v/v, the micelle core radius was found to be 4.71 nm (47.1 Å) with the corresponding hard sphere radius of 8.52 nm (85.2 Å). Further increase in the dilution resulted in the swelling of the micelles with a resultant increase in the total volume percent of the micelle-forming components. This was reflected as an increase in both the core as well as the hard sphere radius of the developed micelles (Table IV).

Cryo-transmission Electron Microscopy

Morphological analysis by cryo-TEM revealed a well-defined spherical nature of the developed zolmitriptan

Table III. Multiangle Dynamic Light Scattering

Angle	Particle size (nm)	PI
50	25.6	0.110
70	25.4	0.105
90	24.2	0.064
110	23.2	0.102
150	22.8	0.112

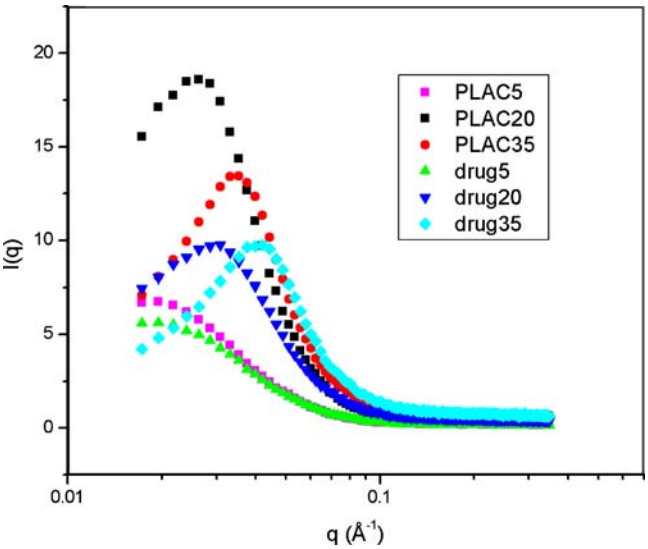

Fig. 1. Intensity graph of Small angle neutron scattering for placebo micellar nanocarrier and zolmitriptan micellar nanocarrier, diluted with D_2O at three ratios viz. Micelle: D_2O ratio 05:95 (PLAC5, Drug5), 20:80 (PLAC20, Drug20) and 35:65 (PLAC35, Drug35).

micelles with a narrow size distribution, which was in compliance with the results of DLS and SANS (Fig. 2A). The size and morphology of both the drug-loaded and the placebo micelles was found to be almost identical (Fig. 2B). Absence of drug precipitation in the micellar dispersion was confirmed by the lack of any large aggregates. Fig. 2C indicates the sample mounted on the grid, as observed under TEM, at a lower resolution. Fig. 2D shows the presence of the perforated carbon support-film as indicated by the letter "F."

Toxicity

The photo micrographs of the rat nasal mucosa are shown in Fig. 3. Fig. 3A, which depicts the negative control, exhibits the orderly arrangement of the cilia on the surface of the mucosa after nasal administration of physiological saline. Similar observations were evident in groups administered with zolmitriptan marketed solution, placebo micellar nanocarrier, and zolmitriptan micellar nanocarrier, respectively. Microscopic effects on the nasal cavities of rats, after administration of various zolmitriptan formulations, have been stated in Table V. Representative photographs of various findings in nasal cavities have been depicted in Fig. 3 (B–D). The results indicate that the developed zolmitriptan formulation did not adversely affect the integrity of nasal mucosa and mucosal cilia. Gross pathological examination showed the absence of alterations in the isolated organs in all the test groups. The effect of zolmitriptan micellar nanocarrier, placebo micellar nanocarrier and the marketed formulation on various hematological parameters, such as hemoglobin content, number of platelets, hematocrit and number of RBCs, and biochemical parameters, such as serum albumin, serum globumin, total protein, urea-nitrogen and creatinine, was studied. The values of various biochemical and hematological parameters have been depicted in Fig. 4A and B. All the values were similar to those observed in case of the negative control group, thus indicating the safety of the developed micellar nanocarrier for nasal administration.

Biodistribution, Brain Localization and Autoradiography Studies

Biodistribution studies revealed that the ^{99m}Tc-zolmitriptan micellar nanocarrier exhibited a significantly higher uptake ($p<0.05$) in the brain when compared with the ^{99m}Tc-zolmitriptan nasal solution and ^{99m}Tc-zolmitriptan I.V. solution at all the time points tested. These results have been depicted in Fig. 5A. Fig. 5B illustrates the gradient distribution of the nasal ^{99m}Tc-zolmitriptan micellar nanocarrier in various regions of the rat brain. Highest concentration of ^{99m}Tc-zolmitriptan was observed within the olfactory area with diminishing distribution in the direction of diencephalon. However, the distribution showed a marked increase in the mid-brain, cerebellum and pons regions of the brain. Analysis at 30, 60 and 120 min. post-administration demonstrated a significantly higher ($p<0.05$) radioactivity in the olfactory bulb as against the other brain sub-parts; however, comparable radioactivity was observed in the mid-brain and cerebellum at the end of 240 min.

Autoradiography studies revealed a distinct and extensive brain distribution of ^{99m}Tc-Zolmitriptanafter intranasal administration, thus supplementing the results of the biodistribution and brain localization studies. Fig. 6(A–D) depicts the representative autoradiograms of the coronal sections of the rat brain after the administration of ^{99m}Tc-zolmitriptan micellar nanocarrier. The radioactivity distribution was observed to be more intense in the regions of olfactory bulb (Fig. 6A), frontal cortex (Fig. 6B), hippocampus (Fig. 6C) and cerebellum (Fig. 6D). The results were similar to those obtained during the brain localization studies. Also, these studies indicated an intense distribution of ^{99m}Tc-zolmitriptan in the glomerular layer, mitral cell layer and the granular cell layer of the olfactory bulb (Fig. 6A).

DISCUSSION

The consortium of excipients employed during formulation resulted in the formation of a stable and reproducible micellar nanocarrier of zolmitriptan. The ability of PF127, a poly (ethylene oxide)-poly (propylene oxide) block copolymer, to self-assemble into polymeric micelles in aqueous systems and to form micellar structures in combination with the latter excipients, has been reported earlier (20–22). TCP acted as an excellent solubilizer for the drug. This formulation component was also included with the intention of enhancing the absorption and penetration of the drug across the nasal mucosa, at the same time lacking mucosal toxicity (23). BA is one of the widely accepted excipients for novel drug delivery systems and was employed for its high drug solubilization capacity and its bacteriostatic activity (24).

Multiangle dynamic light scattering (DLS) technique offers a particular advantage in obtaining high resolution particle size distribution data of complex samples, such as

Table IV. SANS Profile of Micellar Nanocarriers

Sample	Core radius(Å)	Hard sphere radius(Å)
Micelle: D_2O ratio of 35:65 v/v	47.1	85.2
Micelle: D_2O ratio of 20:80 v/v	54.2	110.4
Micelle: D_2O ratio of 05:95 v/v	54.7	134.5

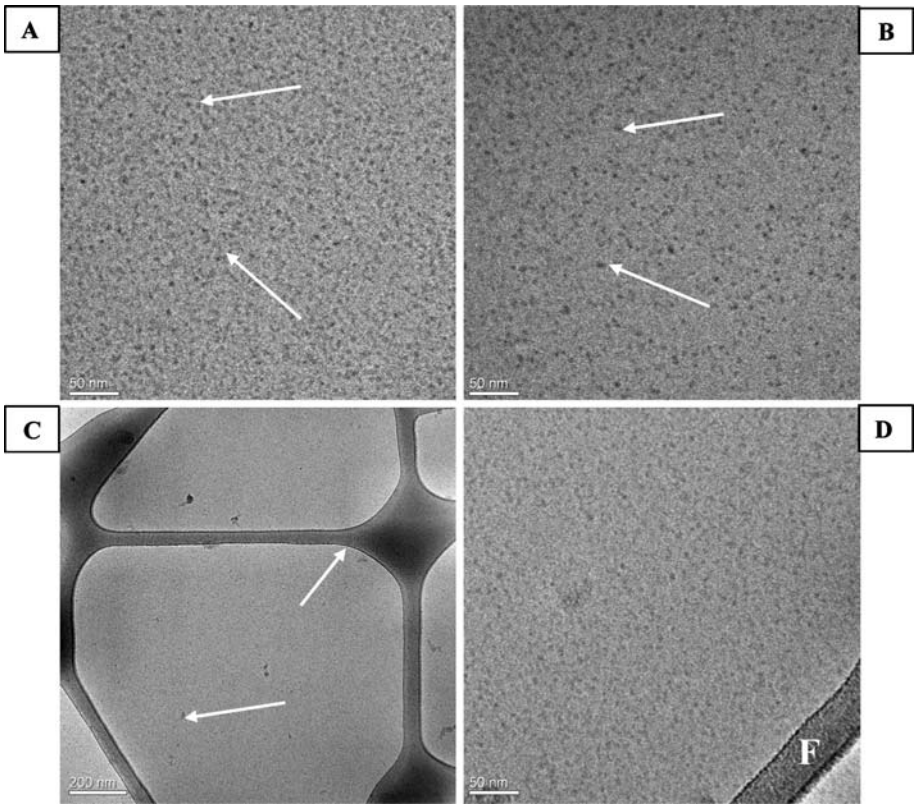

Fig. 2. Cryo-TEM images of A. zolmitriptan micellar nanocarrier, B. placebo micellar nanocarrier, C. image showing micellar nanocarrier at low resolution, D. micellar nanocarriers with perforated carbon film.

micelles, where the formulation components are closely spaced (25). The technique is considered to be more accurate, robust and reproducible when compared to the other particle size analysis techniques. These attributes governed the selection of this technique in assessing the particle diameter and distribution of the formulated micellar nanocarrier.

The block copolymer micelles can be considered as a spherical core shell particle with differing scattering length

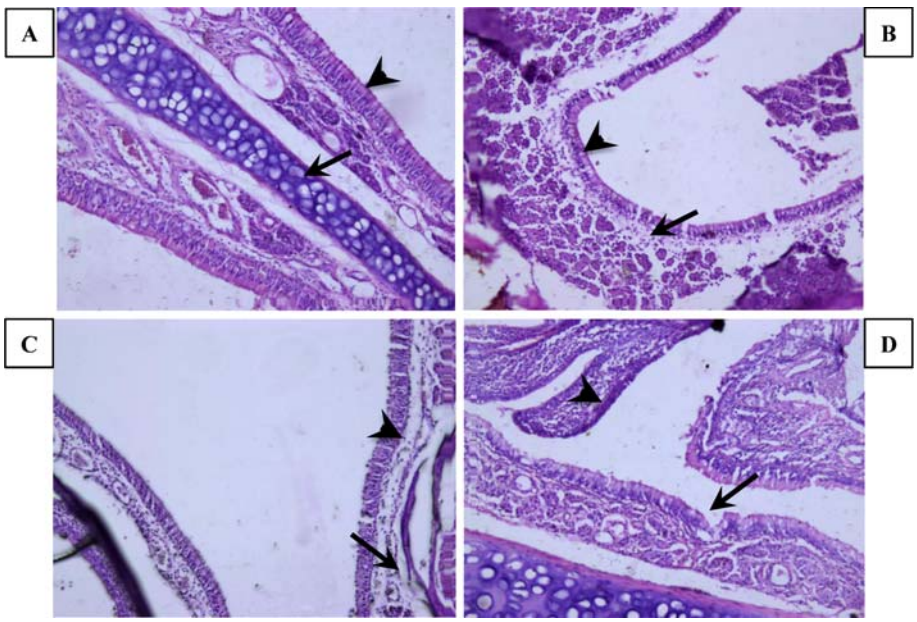

Fig. 3. Photomicrographs of nasal mucosa from control, zolmitriptan and placebo micellar nanocarrier-treated rats. (*A*) control rat showing normal nasal turbinate (arrow) olfactory epithelium with cilia (arrowhead), (*B*) intact olfactory epithelium (arrowhead) with minimum submuosal infiltration (arrow) (*C*) intact olfactory epithelium with submucosal infiltration (arrow) and vacuolated cells (arrowhead), (*D*) mild degeneration in respiratory epithelium (arrow) along with minimal submucosal infiltration (arrowhead).

Table V. Effect of Zolmitriptan Formulations on Nasal Mucosa of Rats Treated Daily for 1, 4, 7 and 28 Days

Formulation	Zolmitriptan Micellar Nanocarrier				Placebo Micellar Nanocarrier				Zolmitriptan Solution			
Days	1	4	7	28	1	4	7	28	1	4	7	28
Rats (Male/Female)	6/6	6/6	6/6	6/6	6/6	6/6	6/6	6/6	6/6	6/6	6/6	6/6
Olfactory Mucosa												
Degeneration												
Minimal severity	0/0	0/1	1/1	1/2	0/0	0/1	0/1	2/1	0/0	1/0	0/1	1/2
Mild severity	0/0	0/0	1/1	1/1	0/0	0/0	0/1	1/1	0/0	1/0	0/1	1/0
Erosion												
Minimal severity	0/0	1/0	1/0	2/1	0/0	1/0	0/1	1/1	0/0	1/0	1/0	1/1
Mild severity	0/0	0/1	1/0	2/2	0/0	0/0	0/1	1/1	0/0	0/1	0/1	0/1
Cell Necrosis												
Minimal severity	0/0	0/0	0/0	1/0	0/0	0/0	0/0	0/1	0/0	0/1	0/1	2/1
Respiratory Mucosa												
Sub-mucosal Infiltration												
Minimal severity	0/0	0/0	1/0	1/1	0/0	0/1	1/1	1/3	0/0	1/0	0/1	2/1
Mild severity	0/0	0/1	1/1	1/2	0/0	0/1	1/0	2/2	0/0	0/1	1/0	0/1
Moderate severity	0/0	0/0	0/0	1/1	0/0	0/0	0/1	0/1	0/0	0/0	0/0	0/1
Degeneration												
Minimal severity	0/0	1/0	1/0	1/2	0/0	1/0	0/1	1/1	0/0	1/0	0/1	1/1
Mild severity	0/0	0/0	0/1	1/0	0/0	0/0	0/1	0/1	0/0	1/0	0/0	0/1
Erosion												
Minimal severity	0/0	0/0	1/0	1/2	0/0	0/1	0/1	2/1	0/0	1/0	0/1	2/1
Nasal Cavity/Mucosa												
Sub-mucosal Infiltration												
Minimal severity	0/0	0/1	1/0	2/2	0/0	0/1	1/1	2/2	0/0	1/0	0/1	2/2
Mild severity	0/0	0/1	1/0	1/1	0/0	0/1	1/0	1/0	0/0	1/0	0/1	2/1
Moderate severity	0/0	0/0	0/0	0/1	0/0	0/0	0/0	1/0	0/0	0/0	0/0	1/1
Goblet Cells												
Minimal severity	0/0	1/0	0/1	1/1	0/0	0/1	0/1	2/2	0/0	1/0	0/1	1/1
Mild severity	0/0	1/0	0/1	1/1	0/0	1/0	1/0	1/0	0/0	0/1	0/1	1/0
Glands												
Minimal severity	0/0	1/0	1/0	1/1	0/0	1/0	1/0	1/1	0/0	0/1	0/1	2/1
Mild severity	0/0	0/0	0/1	0/1	0/0	1/0	0/1	0/1	0/0	0/0	0/1	1/0

Pathological grade: A) For epithelial destruction, 0: NAD: Normal (No abnormality detected), 1: minimal less than 10% pathological changes, 2: mild up to 25% pathological changes, 3: moderate up to 50% pathological changes, 4: severe more than 50% pathological changes B) For Submucosal infiltration (neutrophils and macrophages), 0: NAD: Normal (No abnormality detected), 1: minimal 10–20 cells per hpf (high-power field), 2: mild up to 20–30 cells per hpf, 3: moderate up 30–40 cells per hpf, 4: severe more than 50 cells per hpf.

densities of hydrophobic core and hydrophilic shell. The scattering from shell of the micelle depends on its thickness as well as its scattering length density. Due to high degree of solvation, the scattering length density of the shell will not be significantly different from that of the solvent, and it is difficult to get a unique value of the thickness of the shell when the thickness and contrast of the shell were used as an adjustable parameter. Thus, to limit the number of unknown parameters in the fit, we assumed that, for all practical purposes, the scattering in SANS mainly arises from the core of the micelles. The scattering features exhibited an insignificant decrease in scattering intensity, at low values of q, in the case of drug-loaded samples as compared to the placebo samples, thus implying that the shape of the micelles remained unchanged after incorporating the drug in the formulation.

The results of the cryo-TEM studies confirmed the encapsulation of the drug within the formulated micelles. The images clearly revealed a similar structure for both the placebo and drug-loaded micelles. The absence of drug crystals in the image of the drug-loaded micelles thus verified the incorporation of the drug within the micellar structure.

The similar size of the placebo and the drug-loaded micelles may be attributed to the association between the -NH groups of the drug with the -OH groups of the various formulation excipients (Poloxamer, TPGS, PEG-400, Benzyl alcohol, etc.) through hydrogen bonding. Such an attractive interaction may also account for an altered packing parameter resulting in a more spherical structure of the loaded micelles and hence resulting in a size similar to the placebo micelles. Such an interaction between the drug and formulation excipients accounting for the similar size of the empty and drug-loaded micelles has been reported by other researchers earlier (26).

Toxicological evaluation of the developed formulation was carried out for varying time-spans to evaluate the formulation toxicity subsequent to short-term, intermediate and prolonged administration. The time-span of 28 days was considered to be an adequate period to study the chronic effects of micellar nanocarrier on nasal mucosa and mucosal cilia, since under normal conditions the human ciliated cells exhibit a life of about 4–8 weeks (27), after which the differentiation of the basal cells replaces any damaged and aged cells at the epithelial surface (28).

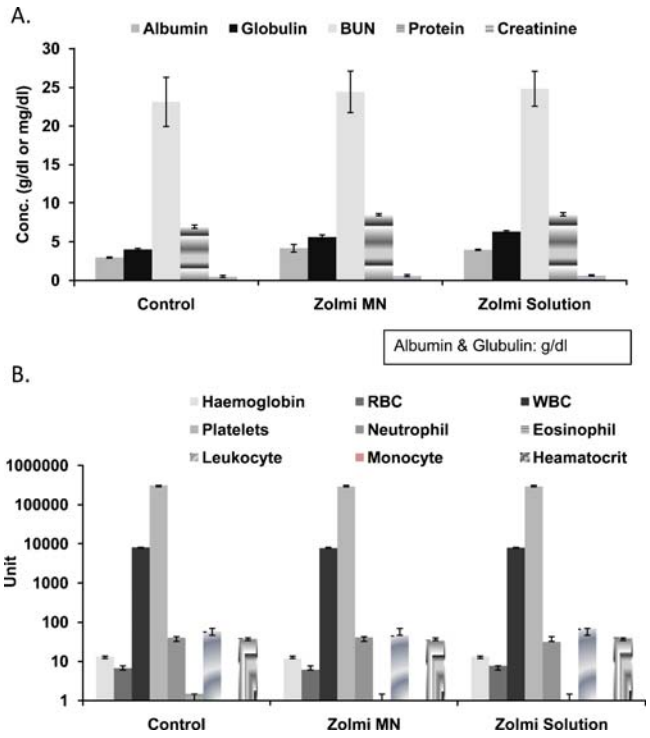

Fig. 4. Serum biochemistry and hematological parameters after 28 days nasal administration of zolmitriptan micellar nanocarriers, placebo micellar nanocarriers and zolmitriptan marketed solution. (Mean±S.D, $n=6$).

In the biodistribution evaluation in rats, a distinctive peripheral organ distribution profile was observed with micellar nanocarriers when compared with the solutions. A high radioactivity in the blood and the brain was observed in the case of the micelles at 30 min. post-administration, whereas the solutions demonstrated a higher activity in blood and liver, respectively. Thus, the micellar nanocarrier exhibited a significantly higher distribution of radioactivity ($p<0.05$) in the brain as compared to the other body organs (data not shown) when compared with the nasal and I.V. solutions of zolmitriptan. The higher brain uptake in the case of the micellar nanocarrier could be attributed to the superior permeation of the nanocarriers across the biological barriers. Micellar nanocarriers have also been reported to transport the drugs to the brain via intracellular and extracellular transport (29) and via the olfactory pathway (30). Although various studies indicating the nose-to-brain transfer of therapeutic moieties using nanocarriers like microemulsions, nanoemulsions, etc. (2,10) have been reported earlier, no report indicates a methodical investigation of the precise pathway involved in the nose-to-brain delivery as well as a regional brain distribution profile.

In the brain localization studies, it was observed that in the first 30 min. post-administration, the drug uptake was restricted to the rostral brain region as evident from the lack of radioactivity in mid-brain (MB), cerebellum (CL), pons (PN) and medulla (MD). Thereafter, an increasing radioactivity distribution was seen in the midbrain and cerebellum regions from 60 to 240 min.

Autoradiography studies helped determine the possible pathway involved in nose-to-brain transfer of ^{99m}Tc-zolmitriptan. Results manifest that after the intranasal administration of the micellar nanocarrier, ^{99m}Tc-zolmitriptan is predominantly transported to the olfactory bulb via the olfactory and trigeminal systems. The transport of the drug complex to the mid-brain and cerebellum occurs via trigeminal pathway. The involvement of these pathways in the nose-to brain transfer of various other molecules has been reported before (31).

The glomerular layer is the site of synaptic contact of the axon terminals of the olfactory receptor neuron with the dendrites of the mitral and tufted cells (32–34), whereas the granule cell layer is rich in granule cells and the axons of mitral and tufted cells (33). Thus, the intense distribution of labelled drug in these areas of the rat brain provides very strong evidence of the targeting of ^{99m}Tc-zolmitriptan to the axon terminals of the olfactory neurons, thus resulting in direct brain targeting of the complex.

Further, results clearly indicated that the ^{99m}Tc-zolmitriptan complex reached the distant brain regions, like the hippocampus and diencephalon, via the olfactory tract, composed of the axons of the mitral and tufted cells, and thereafter reached the olfactory tubercle and frontal cortex, which contains the anterior olfactory nucleus and the amygdaloid body (34). From the frontal cortex, the complex was transferred to other brain regions, such as the caudaputamen, hippocampus and diencephalon, via olfactory transports (35). Also, an intense accumulation of ^{99m}Tc-zolmitriptan in the mid-brain and cerebellum regions, as evident by a dense radioactivity in the cerebellar white matter and the trigeminal tract, strongly suggested the role of the trigeminal system in drug targeting to the brain. Thus, the above studies helped to determine the possible precise pathway involved in nose-to-brain delivery of zolmitriptan from the developed micellar nanocarrier.

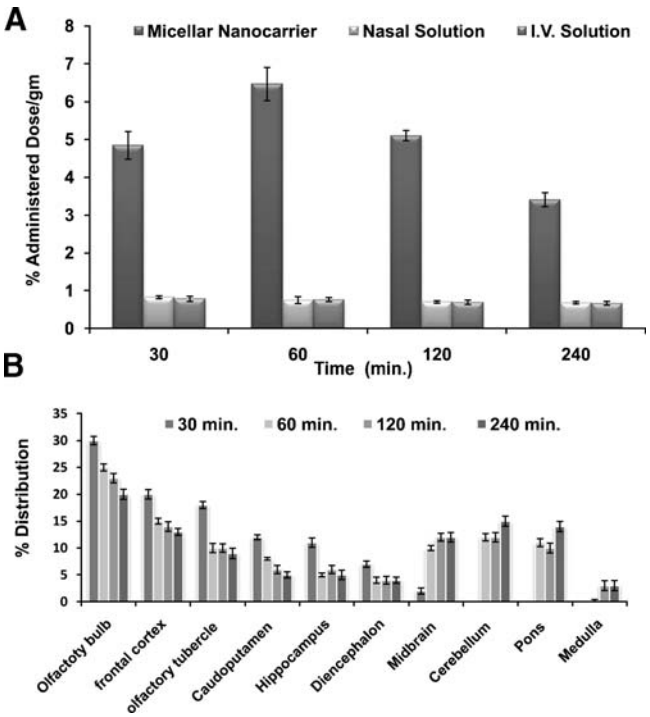

Fig. 5. Biodistribution and brain localization studies, A. Comparative brain uptake profile of micellar nanocarrier, nasal solution and I.V. solution, B. Regional distribution in brain after nasal administration of micellar nanocarrier. (Mean±S.D., $n=6$).

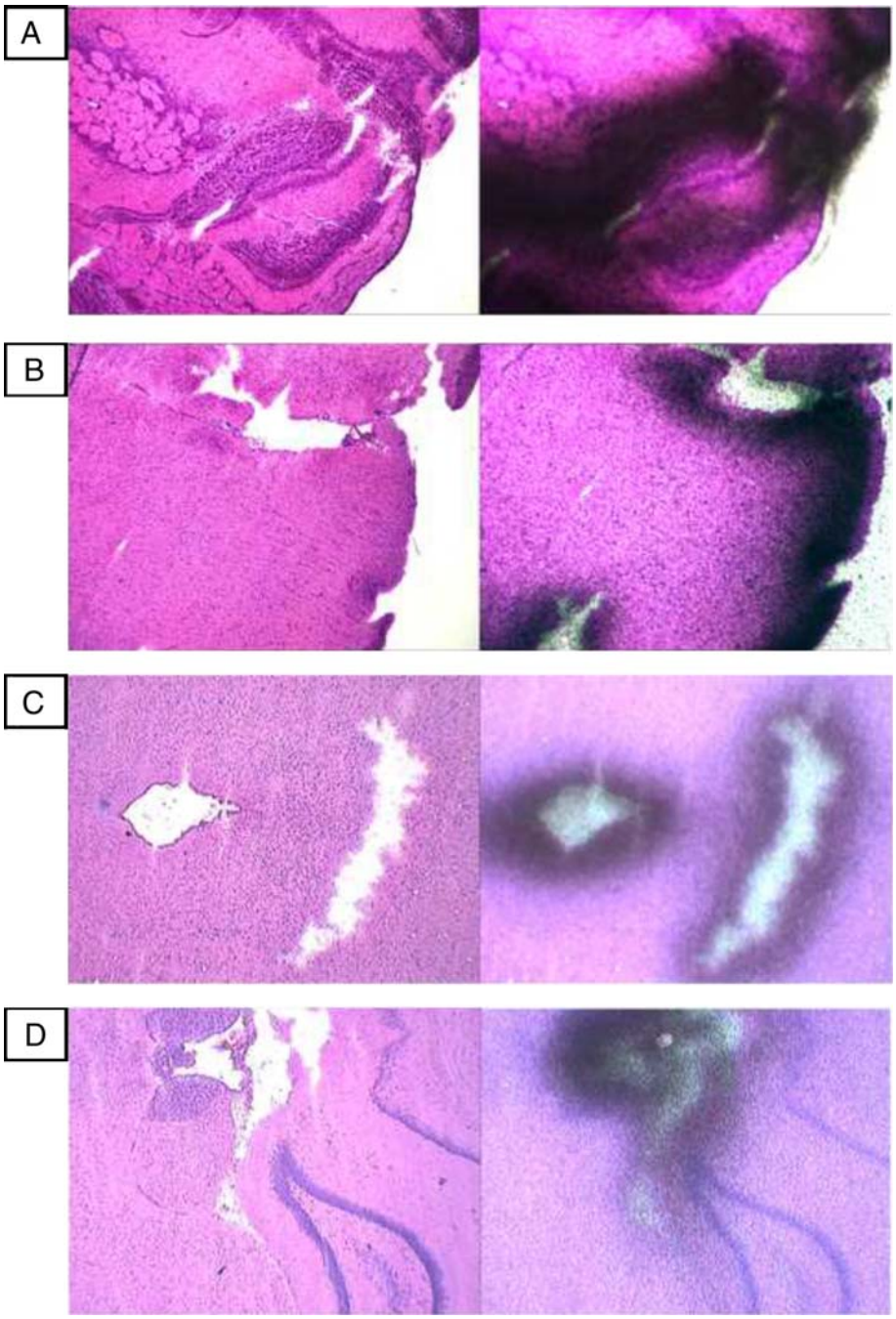

Fig. 6. Representative autoradiogram of rat brain A. Autoradiogram of olfactory lobe, darkened region shows radioactivity distribution. B. Autoradiogram of frontal cortex, darkened region shows radioactivity distribution. C. Autoradiogram of hippocampus, darkened region shows radioactivity distribution. D. Autoradiogram of cerebellum, darkened region shows radioactivity distribution. (Mean±S.D., n=6).

CONCLUSION

Micellar nanocarrier of zolmitriptan was successfully formulated. The spherical nature of the nanocarrier was confirmed using various characterization techniques, like DLS, SANS and cryo-TEM. Toxicity studies indicated the safety of the developed micellar nanocarrier for administration in the nasal cavity. *In vivo* biodistribution studies in rats indicated the superiority of the developed nanocarrier for brain targeting when compared with the results of the intravenous and nasal solutions of the drug. Brain localization and autoradiography studies illustrated the distribution of the drug in various regions of the brain. A possible nose-to-brain transport of ^{99m}Tc-zolmitriptan via the olfactory and trigeminal systems, along with various intracellular, extracellular and axonal pathways, was evident from the dense accumulation of ^{99m}Tc-zolmitriptan in the olfactory region and the cerebellum. Thus, the results indicate the potential of the developed micellar

nanocarrier to rapidly deliver zolmitriptan directly to the brain. Further trials in human volunteers will confirm their clinical application as a new generation anti-migraine therapy.

ACKNOWLEDGEMENTS

The authors are thankful to Archarchem Pharmaceuticals Pvt. Ltd. and Chokhani Pharmaceutical Ltd. for the gift sample of zolmitriptan; Gattefosse, Mumbai, India and BASF India Ltd. for the gift sample of excipients; and Aptar Pharma India Pvt. Ltd., Mumbai, India for the kind gift of Equadel™ Pump. The authors are grateful to Lalit Borde and Dr. Krishanu Ray from Tata Institute of Fundamental Research, Mumbai, India; Prof. Katarina Edwards, Uppsala University, Uppsala, Sweden; and Prof. Ishi Talmon, Haifa, Israel for conducting the cryo-TEM analysis. The authors are thankful to Dr. P. A. Hassan, Dr. V. K. Aswal for DLS and SANS analysis, and Dr. Tanuja Shet for authoradiography Studies. Ratnesh Jain is thankful to the Board of Research in Nuclear Sciences (Sanction No. 2006/35/11/BRNS), Department of Atomic Energy, Gov't of India, for providing the funding to execute the research.

REFERENCES

1. Tepper SJ, Rapoport AM. The triptans: a summary. CNS Drugs. 1999;12:403–17.
2. Vyas TK, Babbar AK, Sharma RK, Misra A. Intranasal mucoadhesive microemulsions of zolmitriptan: preliminary studies on brain-targeting. J Drug Target. 2005;13:317–24.
3. Rao BM, Srinivasu MK, Sridhar G, Rajender Kumar P, Chandrasekhar KB, Islam A. A stability indicating LC method for zolmitriptan. J Pharm Biomed Anal. 2005;39:503–9.
4. Rolan PE, Martin GR. Zolmitriptan: a new acute treatment for migraine. Expert Opin Investig Drugs. 1998;7:633–52.
5. Patel SR, Zhong H, Sharma A, Kalia YN. Controlled non-invasive transdermal iontophoretic delivery of zolmitriptan hydrochloride *in vitro* and *in vivo*. Eur J Pharm Biopharm. 2008;72:304–9.
6. Bigal ME, Bordini CA, Antoniazzi AL, Speciali JG. The triptan formulations: a critical evaluation. Arq Neuro-Psiquiatr. 2003;61: 313–20.
7. Goadsby PJ, Yates R. Zolmitriptan intranasal: a review of the pharmacokinetics and clinical efficacy. Headache. 2006;46:138–49.
8. Yates R, Nairn K, Dixon R, Seaber E. Preliminary studies of the pharmacokinetics and tolerability of zolmitriptan nasal spray in healthy volunteers. J Clin Pharmacol. 2002;42:1237–43.
9. Tepper SJ, Donnan GA, Dowson AJ, Bomhof MAM, Elkind A, Meloche J, *et al.* A long-term study to maximize migraine relief with zolmitriptan. Curr Med Res Opin. 1999;15:254–71.
10. Vyas TK, Babbar AK, Sharma RK, Singh S, Misra A. Intranasal mucoadhesive microemulsions of clonazepam: preliminary studies on brain targeting. J Pharm Sci. 2006;95:570–80.
11. Torchilin VP. Micellar nanocarriers: pharmaceutical perspectives. Pharm Res. 2007;24:1–16.
12. Simon M, Wittmar M, Kissel T, Linn T. Insulin containing nanocomplexes formed by self-assembly from biodegradable amine-modified poly (Vinyl Alcohol)-Graft-Poly (L-Lactide): bioavailability and nasal tolerability in rats. Pharm Res. 2005;22:1879–86.
13. Quadir M, Zia H, Needham TE. Toxicological implications of nasal formulations. Drug Deliv. 1999;6:227–42.
14. Schillen K, Brown W, Johnson RM. Micellar sphere-to-rod transition in an aqueous triblock copolymer system. A dynamic light scattering study of translational and rotational diffusion. Macromolecules. 1994;27:4825–32.
15. Almgren M, Edwards K, Karlsson G. Cryo transmission electron microscopy of liposomes and related structures. Colloids Surf A. 2000;174:3–21.
16. Nabar SJ, Jain R, Patravale VB. Preparation, quality control and stability of 99mTc-Zolmitriptan nanocarrier. Ind J Nucl Med. 2008;23:77.
17. Thorne RG, Emory CR, Ala TA, Frey WH. Quantitative analysis of the olfactory pathway for drug delivery to the brain. Brain Res. 1995;692:278–82.
18. Thomas GH, Hartman JA, Seiden LS. Rapid method for the regional dissection of the rat brain. Pharmacol Biochem Behav. 1980;13:453–6.
19. Paxinos G, Watson C. The rat brain in stereotaxic coordinates. San Diego: Academic; 1998.
20. Oh KT, Bronich TK, Kabanov AV. Micellar formulations for drug delivery based on mixtures of hydrophobic and hydrophilic Pluronic® block copolymers. J Control Release. 2004;94:411–22.
21. Ivanova R, Lindman B, Alexandridis P. Effect of pharmaceutically acceptable glycols on the stability of the liquid crystalline gels formed by Poloxamer 407 in water. J Colloid Interface Sci. 2002;252:226–35.
22. Gao Y, Li LB, Zhai G. Preparation and characterization of Pluronic/TPGS mixed micelles for solubilization of camptothecin. Colloids Surf B. 2008;64:194–9.
23. Xie Y, Wei L, Cao S, Jiang X, Yin M, Tang W. Preparation of bupleurum nasal spray and evaluation on its safety and efficacy. Chem Pharm Bull. 2006;54:48–53.
24. Hammad MA, Müller BW. Solubility and stability of clonazepam in mixed micelles. Int J Pharm. 1998;169:55–64.
25. Bryant G, Thomas JC. Improved particle size distribution measurements using multiangle dynamic light scattering. Langmuir. 1995;11:2480–5.
26. Mackeben S, Muller M, Muller-Goymann CC. The influence of water on phase transitions of a drug-loaded reverse micellar solution into lamellar liquid crystals. Colloid Surf A. 2001;183–185:699–713.
27. Herzon FS. Nasal ciliary structural pathology. Laryngoscope. 1983;93:63–7.
28. Rautianen M, Muutinen J, Kiukaaniemi H, Collan Y. Ultrastructural changes in human cilia caused by the common cold and recovery of ciliated epithelium. *In vivo* results in animals. Drug Invest. 1994;8:127–33.
29. Meaney CM, O'Driscoll CM. A comparison of the permeation enhancement potential of simple bile salt and mixed bile salt: fatty acid micellar systems using the CaCo-2 cell culture model. Int J Pharm. 2000;207:21–30.
30. Illum L. Transport of drugs from the nasal cavity to central nervous system. Eur J Pharm Sci. 2000;11:1–18.
31. Thorne RG, Pronk GJ, Padmanabhan V, Frey WH. Delivery of insulin-like growth factor-I to the rat brain and spinal cord along olfactory and trigeminal pathways following intranasal administration. Neuroscience. 2004;127:481–96.
32. Kanayama Y, Enomoto S, Irie T, Amano R. Axonal transport of rubidium and thallium in the olfactory nerve of mice. Nucl Med Biol. 2005;32:505–12.
33. Haberly LB, Price JL. Association and commissural fiber systems of the olfactory cortex of the rat: I. Systems originating in the piriform cortex and adjacent areas. J Comp Neurol. 1978;178:711–40.
34. Fechter LD, Johnson DL, Lynch RA. The relationship of particle size to olfactory nerve uptake of a non-soluble form of manganese into brain. Neurotoxicology. 2002;23:177–83.
35. Sakane T, Akizuki M, Yoshida M, Yamashita S, Nadai T, Hashida M, *et al.* Transport of cephalexin to the cerebrospinal fluid directly from the nasal cavity. J Pharm Pharmacol. 1991;43:449–51.